CrystEngComm

ROYAL SOCIETY OF CHEMISTRY

HIGHLIGHT

View Article Online
View Journal | View Issue

Cite this: *CrystEngComm*, 2021, **23**, 7916

Crystal engineering of nanomaterials: current insights and prospects

Marion Görke and Georg Garnweitner *

Received 5th May 2021,
Accepted 1st July 2021

DOI: 10.1039/d1ce00601k

rsc.li/crystengcomm

The rather loosely defined field of crystal engineering offers a wide variety of approaches towards the precise design of nanocrystals for different applications. Thereby, inorganic nanomaterials have been in the focus of research due to their highly interesting characteristics, and the possibility to obtain fascinating structures and morphologies at the smallest size scales. Despite great progress and a steady increase in complexity of the synthesized materials, the targeted preparation of nanocrystals however is still only feasible to a limited extent. Further intensification of the cross-disciplinary exchange of results and insights in nanocrystal engineering on a joint platform like CrystEngComm can accelerate the development of unifying concepts in crystal design and an understanding of structure–property relations. Therefore, this article aims to present the diversity of nanocrystal engineering research, by highlighting some of the most intriguing research results over the past few years.

Introduction

For many years, CrystEngComm has been featuring research articles and communications on the formation and growth of inorganic nanomaterials. Whilst the background of the journal in the field of crystal engineering seems to logically and naturally set the scope to all works devoted to the controlled formation of crystalline materials, the actual definition of crystal engineering is much narrower, as "the design and synthesis of molecular solid state structures with desired properties, based on an understanding and use of intermolecular interactions".[1] Hence, crystal engineering of inorganic nanomaterials is not covered by this definition, and moreover does not involve the design of crystal structure

---

Technische Universität Braunschweig, Institute for Particle Technology and Laboratory for Emerging Nanometrology, 38104 Braunschweig, Germany. E-mail: g.garnweitner@tu-braunschweig.de

Marion Görke

Marion Görke received a master's degree in chemistry at the Technische Universität Braunschweig, Germany, in 2020, and started her PhD in Georg Garnweitner's group at the Institute for Particle Technology, Technische Universität Braunschweig, Germany, within the Hannover School for Nanotechnology programme. She gained first experiences in the synthesis and functionalization of nanoparticles at the University of Utah, USA, during a stay abroad in 2018/19. Currently the major topic of her PhD work is the synthesis, functionalization and controlled self-assembly of magnetic nanoparticles.

Georg Garnweitner

Georg Garnweitner received a Diploma in Technical Chemistry at Vienna University of Technology, Austria, in 2003 and then moved to the Max Planck Institute of Colloids and Interfaces, Potsdam, Germany, where he obtained his Ph.D. in Colloids Chemistry in 2005. He was appointed as Professor at Technische Universität Braunschweig, Germany, in 2007. His research is centered on the synthesis of inorganic nanoparticles and nanomaterials, surface modification and functionalization, as well as diverse application fields of nanostructured materials ranging from batteries to biomedicine. From 2013 to 2020 he served as Associate Editor of CrystEngComm, mainly handling manuscripts in the nanomaterials field.

and properties *via* adjustment of the individual building units as is possible for supramolecular materials.

Whilst a clear and concise definition is lacking, crystal engineering of nanomaterials in a broader sense has become highly important for many research fields. As an example, plasmonic nanomaterials possess optical properties that can be tailored *via* crystal properties and morphologies, and complex structures like nanostars are broadly used – without in-depth understanding of crystal formation and growth processes, the controlled preparation and adjustment of such materials is hardly possible. Moreover, *e.g.* the development of catalysts for fuel cell applications requires the proper design of noble metal nanocrystals, to achieve optimal performance while minimizing critical material costs. As another example, semiconductors can be tuned in their electronic properties by adjusting crystal size and shape, and combined in heterostructures with crystallographically defined contacts for their further enhancement. Whilst for each material system, the specific mechanisms of formation and growth and the implications of crystal characteristics on application-oriented properties are different, the exchange of concepts and mechanistic insights not just within one class of material or one application field, but also between the systems has proven to be highly beneficial and important to foster their advancement. Crystal engineering can act as unifying platform for such works, enhancing cross-disciplinary and cross-system interaction for mutual benefit.

The goal of this Highlight article is to present the diversity of crystal engineering concepts for inorganic nanomaterials, and shed light on several aspects that according to our opinion make up crystal engineering in its broader sense. Thereby, our scope is not to give a comprehensive overview, but to point out particularly interesting examples of research in the last few years, with a special focus on the discussion of works published in CrystEngComm as one prime forum for crystal engineering studies.

1. Control of morphology and phase

From the first report on the observation of nanoparticles in the literature[2] to the present day, research on the controlled growth and design of nanocrystals has greatly advanced. For some systems, especially metals, the synthesis of monodisperse nanoparticles is long known[3] and more sophisticated formation strategies and products have been pursued in the last decades. Thereby, research has largely moved on from synthesizing simple spheres to more and more complex structures and systems. These systems are mostly designed to have the optimum properties for their individual application. And even though the field of crystal engineering started off with trial and error investigations, a multitude of concepts have been presented to enable a more rational control of the desired characteristics and properties for specific systems. In the following sections we introduce some remarkable achievements in the design and growth of nanocrystals with specific morphology and phase, categorized mainly by their physical appearance.

1.1 Systematic morphology control

In many cases the morphology of a nanocrystal can be systematically tuned by varying a single parameter in the synthesis procedure. One broadly applicable, established strategy to control the morphology during synthesis is the addition of surfactants.[4,5] Whilst for metal nanocrystals there have been many reports on the systematic variation of nanocrystal morphologies *via* reduction processes,[6–8] for other materials the control of morphology is substantially more difficult. As one impressive example for metal oxides, Kang *et al.* systematically investigated the usage of polyvinylpyrrolidone (PVP) to manipulate the morphology of Co_3O_4 nanocrystals in the additional presence of oxalate ions (Fig. 1).[9] It was shown that the concentration of PVP in the hydrothermal synthesis had a main influence on the shape of the crystals. In contrast, the concentration of oxalate ions hardly had any effect on the morphology but determined the size of the resulting nanocrystals.

This illustrates the great versatility of surfactants in adjusting the properties of nanocrystals, of which one still is only beginning to have a general and rational understanding.

Not only surfactants, but also the reaction medium itself can have a strong impact on the morphology of nanocrystals.[10] Morphology control can be achieved without the usage of added surfactants if the medium itself interacts with the forming product, as our research group has reported for the synthesis of aluminum zinc oxide (AZO) nanocrystals.[11] Thereby the shape of the AZO particles was varied from rods to spheres by a change of the used solvent: spheres were formed in benzylamine, whereas rods were obtained in benzyl alcohol. In these reactions the respective medium interacted with the surface of the forming nanocrystals, with benzyl alcohol blocking growth in the *h* and *k* crystal directions, as was elucidated by performing the synthesis in mixtures of the solvents. The crystal size could additionally be adjusted *via* the precursor concentration, as well as the amount of doped aluminum, to tailor the optical properties and band gap of the nanocrystals. Also, combinations of additives well-known for morphological influence such as polymers or urea, and

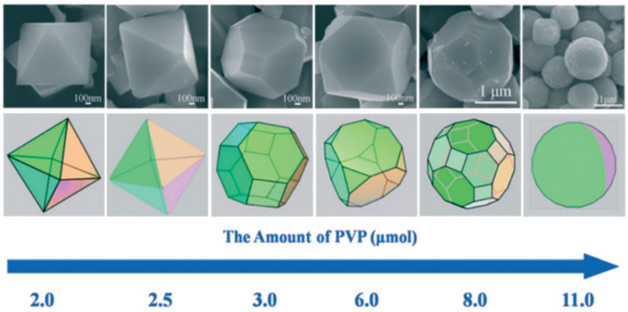

Fig. 1 The morphology of the Co_3O_4 nanocrystals could be tuned from octahedra to corner-truncated octahedra, corner-truncated cubes, globate polyhedra and microspheres under the influence of PVP in the additional presence of oxalate. Reproduced from ref. 9 with permission from the Royal Society of Chemistry.

variations in reaction medium composition are frequently employed for adjusting the morphology of inorganic nanostructures. Whilst in many cases, the variation of more complex morphologies such as urchin-like structures has been demonstrated, thorough investigations revealed that this is typically not due to shape changes of the individual nanocrystals but rather different arrangements of nanocrystals into larger structures.[12]

In some cases, metal doping can also have a strong effect on the morphology of nanocrystals, as was elucidated in detail in fascinating studies *e.g.* for the formation of MoS_2 nanoplatelets that show a drastic change in morphology when smallest amounts of Co^{2+} or Ni^{2+} are introduced.[13] Due to the high relevance of such chalcogenide nanostructures for electrocatalysis, a great deal of research has been devoted to achieving a further understanding of this precise morphology effect.[14] For many other materials, similar effects have been discovered, as for example presented by Chen *et al.*[15] for the synthesis of BiOBr nanosheets. The formation is disrupted by the addition of Pd, leading to irregular and rough edges. This unwanted behavior could be prevented by a previous doping of the nanosheets with La. In this case the morphology is not altered, and the Pd/La-codoped nanosheets showed enhanced electronic properties.

Many materials show strong differences in the surface energies and strength of interactions with molecules for their individual crystal planes. Thus, to achieve highest activity *e.g.* in catalysis, nanocrystals possessing a maximized content in the most active planes are desired. Crystal plane control strives to conceive and synthesize crystals with defined ratios of the different planes, but despite numerous reports on the adjustment of morphology and preparation of nanocrystals with maximized high-energy facets, rational crystal plane control is still at its infancy. Ideally, in such studies modelling and experiments go hand in hand to achieve materials with highest performance. Zhou *et al.* have recently presented such a combined study for ZnO, achieving significant enhancement of catalytic activity for pyramidal ZnO nanorods with exposed {101} faces compared to prismatic nanorods.[16]

1.2 Complex morphologies

A fascinating topic in nanocrystal engineering is the preparation of complex shapes, often resembling macroscale objects. Because materials possess strongly different growth behavior and growth directions, and ligands can be utilized to influence growth in manifold ways, the possibilities for the formation of different shapes are immense.

Among the most investigated morphologies are the flower-like and star-like shapes. Thereby, assembled structures of peculiar-shaped primary crystals are of special interest. Already in 2009, Yu *et al.* presented a solvothermal route to prepare trigonal selenium micro-flowers.[17] To control the physical appearance of the flowers, they used NH_4Cl and different volume ratios of ethanol and water. By increasing the amount of ethanol in the synthesis they were able to mimick a "blossoming process" from bud-like to full blossom structures.

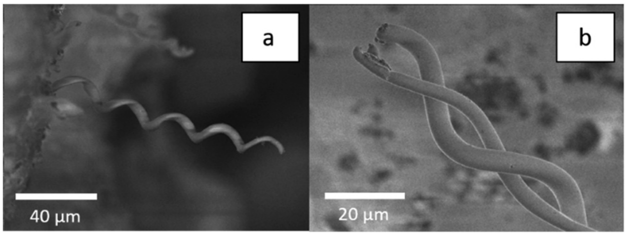

Fig. 2 FESEM images of γ-Dy_2S_3 whiskers; (a) single helical whisker; (b) example of a whisker split into two separate helices. Reproduced with slight adaptation from ref. 19 with permission from the Royal Society of Chemistry.

But also more recent publications on flower-like structures show that the variation of reaction conditions is key to morphological control. Thakur *et al.* recently showed the solvothermal synthesis of flower-like structures composed of ZnO nanorods, as well as nanosheets *via* the reaction of a coordination polymer in organic solvents.[18] By varying the used solvent they created 1D nanorods that then assembled into fascinating 3D nanoflowers with highly versatile characteristics. Key in this process were the different boiling temperatures of the solvents and therefore the different reaction temperatures. The reaction time only affected the aspect ratios of the 1D rods. When the pH value of the reaction mixture was changed, 2D nanosheets instead of nanorods were formed that also assembled into flower-like structures. Due to the different "building blocks", the physical appearance of both flower types however showed a huge difference.

Another complex approach towards sophisticated morphologies is the formation of helical single-crystal whiskers, as presented by Nikolaev *et al.* in a very recent contribution (Fig. 2).[19] The authors realized γ-Dy_2S_3 whiskers *via* isothermal flux evaporation from a high-temperature SnS-Dy_2S_3 melt in the presence of graphite particles, and proposed a mechanism for the growth process. The formation was identified to proceed *via* two steps: first, a three-phase interface is formed, consisting of growing crystal, graphite particle and supply medium, that is needed to induce the axial screw dislocation of the crystals, and second, cooperative evaporation of Dy_2S_3 with SnS occurs. The second step resulted in the formation of intermediate $Dy_2S_3{\cdot}n$ SnS clusters, which ensured the material supply for the growing whisker, since pure rare earth sulfides usually have a negligible vapor pressure even at high temperatures.

1.3 Hollow structures

Crystal engineering can also involve the defined transformation of a crystal. A particularly intriguing case is the formation of hollow crystals, which are of high relevance *e.g.* for catalysis and electrochemistry, since the inside of these hollow structures features active sites as well. Whilst hollow single crystals can be directly grown, for example in a gel matrix,[20] most works rather follow a multistep synthesis approach. Thereby, the template-free synthesis typically involves the transformation of the initially formed crystal to a hollow structure, whilst the application of templates allows the realization of arbitrary morphologies.[21]

As templates, usually preformed nanoparticles of different sizes and shapes are utilized, which can be obtained *via* an easily controllable synthesis. In the next step the desired material nucleates at the surface of the template, and grows to a uniform or nanostructured shell. Afterwards the template is removed and only the hollow nanocrystal remains. Whilst not in all cases, the resulting nanostructure is single-crystalline, the defined facets of the template nanocrystal often are well-preserved in the resulting product. As one such example, Zhao *et al.* showed an interesting approach towards the synthesis of trimetallic PtPdCu hollow alloy octahedra *via* the usage of Cu_2O octahedra as sacrificial templates (Fig. 3).[22] The thickness of the wall could be controlled by the used amount of precursors, which gives an easy and highly effective way to tailor the product properties. Due to the hollow and porous structure, the octahedra showed high catalytic efficiency as well as enhanced durability and stability.

Also the preparation of hollow metal oxides has been presented, for example the template-free one-pot synthesis of hollow Cu_2O nanocages.[23] In this case the nanocrystals were formed *via* precipitation and reduction of $Cu(OH)_2$, whilst sodium dodecyl sulfate (SDS) was used as shape-directing and protecting agent. The selective attachment of SDS to the edges and corners of the Cu_2O nanocrystals resulted in a facet-selective acid etching, which resulted in the formation of hollow octahedron-shaped nanocages. In further experiments the obtained nanocages showed enhanced catalytic performance in the thermal decomposition of ammonium perchlorate compared to solid Cu_2O nanocrystals.

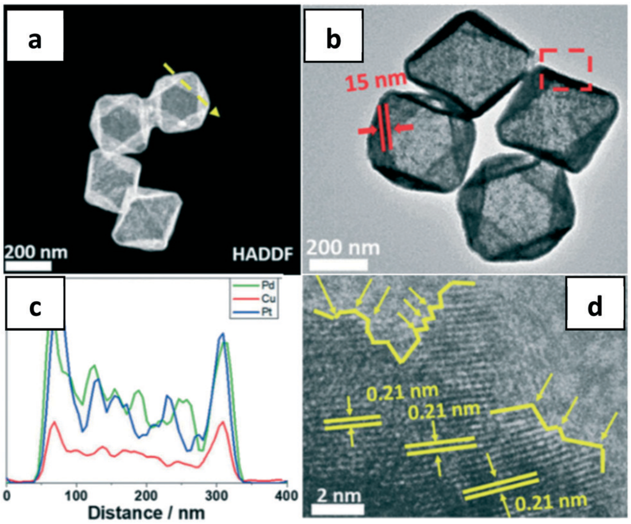

Fig. 3 (a) HAADF-STEM image of PtPdCu hollow octahedra; (b and d) TEM images of PtPdCu hollow octahedra; (c) EDX line scanning of the PtPdCu hollow octahedra; in the images the hollow structure and high crystallinity can be seen. Reproduced with slight adaptation from ref. 22 with permission from the Royal Society of Chemistry.

Another template-free approach was made by Yang *et al.* with the synthesis of Co_3O_4 hollow spheres consisting of nanoflakes.[24] These structures were formed *via* self-assembly of single Co_3O_4 flakes and the impact of the Kirkendall effect, but became unstable over time resulting in sheet-like structures. The nanosheets showed a thickness of ~10 nm whereas the final hollow spheres reached up to 3 μm.

All of the aforementioned works show examples of how the hollow structure enabled an enhancement in catalytic and electrochemical properties. An additional aspect is the reduced material consumption. Hollow structures require less material than their dense counterparts, which is especially important in fields where the required material is either extremely rare or highly toxic.

1.4 Concave structures

An equally fascinating topic is the formation of concave nanocrystals that apparently contradict classical crystallization theories. Concave structures provide similar advantages in catalysis and electrochemical processes as hollow structures, like higher efficiency and less material consumption.[25] A typical formation strategy is the facet-specific dissolution of cube-shaped nanocrystals, but also the implementation of cavities in spheres can be applied. For the latter, an example was given by Rouet *et al.* with the synthesis of silica-based patchy particles.[26] To create concave cavities on the surface, polystyrene beads were first attached to the newly formed silica cores, and after further growth of the silica particles they were removed. Alternatively, the direct formation of concave nanocrystals is possible *via* the selective binding of organic ligands that block further growth to certain sites during synthesis. An example of this approach was presented by Li *et al.* for the preparation of single-crystalline PtCo concave nanooctahedra.[27] The concave structure of these nanocrystals was achieved by using iminodiacetic acid as a structure-guiding agent that caused both the octahedral morphology and the concave nature of the product by chelation of the metal ions. Due to the exposure of the highly active {110} facets these nanocrystals showed greatly enhanced electrocatalytic activity.

This short overview of different types of complex nanocrystal morphologies that have been heavily investigated in the last years illustrates how new structures and morphologies of nanocrystals can give rise to enhanced properties and new applications. But even though this seems highly promising, it is still a huge challenge to create these new structures in a reproducible and scalable synthesis, and most works still follow an empirical approach. This is why a deeper understanding of morphology control and nanocrystal formation is necessary. A promising approach could be the systematic investigation of the relation between morphology and phase of a material.

1.5 Phase control

As described in the sections above, the performance of nanocrystals can be optimized for individual applications by adapting their morphology and composition. This is also true for their phase, where certain phases, for example, show higher catalytic efficiencies and stabilities than others[28] or improved optoelectronic features.[29] Whilst there are numerous studies on the preparation of different phases of a material under different synthesis conditions, detailed insights into the mechanisms of formation of a particular phase are largely lacking, and also the systematic study of controlling and varying the phase composition of nanoparticle products are rare.

A highly illustrative example in this direction was given by Panciera *et al.*, who grew GaAs nanowires with a self-catalyzed molecular beam epitaxy strategy using molten gallium and arsenic on a SiC membrane.[30] During this process it was possible to control the formed phase and also the morphology by adjusting the contact angle of the starting materials through regulation of the incoming material fluxes. The fluxes were varied in composition as well as the amount of starting material. Less material resulted in a small contact angle, more material in a wider angle. The growth was traced and filmed with an electron microscope. From these findings, Panciera *et al.* derived a phase diagram to illustrate the relation of contact angle and surface energy during the growth process (Fig. 4). Thereby, transitions from tapered zinc blende (ZB) nanowires at small contact angles to vertical wurtzite (WZ) structures at intermediate contact angles and back to ZB nanowires with wetted truncated edges at large contact angles were demonstrated.

This is a good example of how a certain morphology can determine the phase of a nanocrystal, since the crystal follows a given shape. Even though this case shows that growth conditions can simultaneously affect phase and morphology, in most other examples in the literature only one of these properties is adjusted and studied. Since the phase of a nanocrystal is determined by the unit cell, most approaches towards phase control are directed towards the synthesis itself. Typical approaches involve the use of additives,[31] regulation of the temperature[32] or a combination of different parameters.[33]

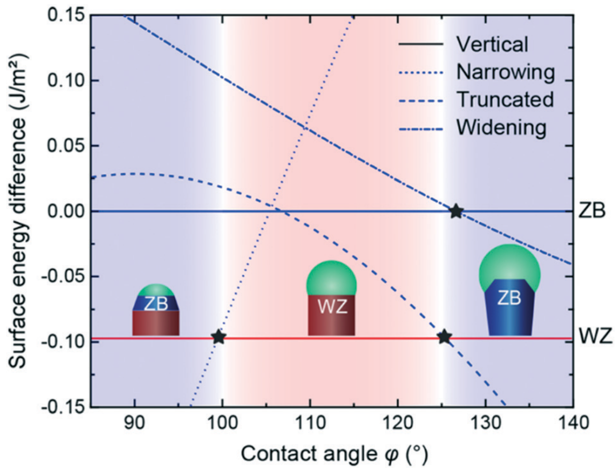

Fig. 4 Model for the morphology and phase control of GaAs nanowires grown *via* self-catalyzed molecular beam epitaxy *via* molten Ga and As. Reproduced from ref. 30 with permission from the American Chemical Society.

Even for simple metal oxides, the control of phase composition remains challenging. In particular, nonaqueous and nonhydrolytic synthesis approaches are increasingly applied also at larger scales as they lead to highly uniform products, but bear little straightforward possibility for the adjustment of product properties, partially also because the mechanisms of formation are still not fully understood. Hence, only few examples have been reported for precise adjustment of the phase composition *via* these methods. For ZrO_2 as an important transition metal oxide with numerous applications, we presented the formation of nanoparticles with controlled ratio of the monoclinic *vs.* the tetragonal phase, ranging from 80% monoclinic phase content to purely tetragonal depending on the synthesis temperature, whilst keeping the particle size relatively constant at about 4–5 nm.[34] By switching the material of the reaction vessel as well as performing calcination experiments, the formation of the different phases could be attributed to the different nucleation and growth kinetics of the two phases. In a subsequent study, the obtained phase composition and crystallite sizes were modeled using population balance equations, revealing strongly different growth rates between the two phases, whilst phase transition occurs with a certain size-dependent probability throughout the synthesis.[35] In a later study, also the chemical nature of the used reaction medium and its binding to the nanocrystal surface were identified to play a major role in the determination of the phase of the forming nanocrystals.[36]

An alternative approach towards phase control is the induction of a precise phase transition process after synthesis and deposition. For this route, Yu *et al.* gave an exceptional example with a method to prepare thermodynamically stable $1T'\text{-}MoX_2$ (X = S, Se) crystals.[37] The authors describe the synthesis of $1T'\text{-}MoS_2$ followed by the laser-induced transformation to $2H\text{-}MoS_2$. In group-VI transition metal dichalcogenides, the 1T phase possesses octahedral coordination of the Mo atoms, whilst the 2H phase shows trigonal prismatic coordination. Since the 1T-phase has usually a more metallic characteristic, while the 2H-phase is a semiconductor, this subsequent phase transition gives rise to new opportunities in electrochemical applications.

2. Composite nanocrystal materials

A strongly applied alternative approach to greatly adapt materials properties or even create novel properties is the combination of two or more phases with same or different composition. In addition to the characteristics of the individual nanocrystals, also the nature and structure of the interface between the different phases is decisive for the properties of such a composite material.

The most straightforward design of a composite nanocrystal material, containing a nanostructure composed of two or more crystalline phases with defined arrangement, involves the growth of a second material on the surface of a nanocrystal to form an encapsulating shell. Thereby, protection against chemical or thermal degradation can be achieved, as well as *e.g.* an enhancement of optical properties due to the prevention of surface quenching effects. In other cases, the resulting properties result from the interaction of the core and shell material, often going beyond linear combination effects. Here, different classes of materials are often combined as one type of heterojunction to achieve superior properties. This concept has been driven even further by applying more layers or altering the underlying morphology.

A nice example of spherical core–shell structures was recently presented by Sun *et al.* with the formation of phase-selective spherical Au@CuS nanocrystals.[38] The phase was controlled by varying the stoichiometry to obtain either cubic digenite or hexagonal covellite phases, which determined the free hole concentration in the shell and thus, the plasmon resonance frequency. The thickness of the shell on the other hand only affected the refractive index and therefore induced a red-shift of the plasmon peak. The quantum yield could be increased by increasing the size of the Au core. This could be adjusted in a rational way, due to the stepwise synthesis approach, with Au-nanoparticles acting as seeds for the CuS shell. Overall, this work showed an enhanced optical tunability and multimodality of the core–shell system, which allows the selective excitation of different optical transitions for enhanced photothermal and photocatalytic efficiencies.

A remarkable finding was presented by Takahashi *et al.* for realization of a next level of complexity in core–shell structures, in the form of double-shell structures (Fig. 5).[39] To synthesize Ag@FeCo@Ag core–shell–shell structures, the precursors for the individual layers were added stepwise into the reaction mixture. The particle formation however did not take place in a stepwise manner. Instead, the authors observed a simultaneous reaction, starting once all the precursors were present in the reaction solution. Whilst a double-shell structure nevertheless was obtained, this led to the formation of outer shells with a gradient composition rather than clearly distinct shells, which was determined using EDS and HAADF-STEM. The silver core was identified to act as a catalyst to reduce the iron and cobalt ions, which resulted in a concentration gradient of Fe and Co due to their different reduction potentials. The outer silver shell was the result of phase separation, since silver is not miscible with iron and cobalt.[39]

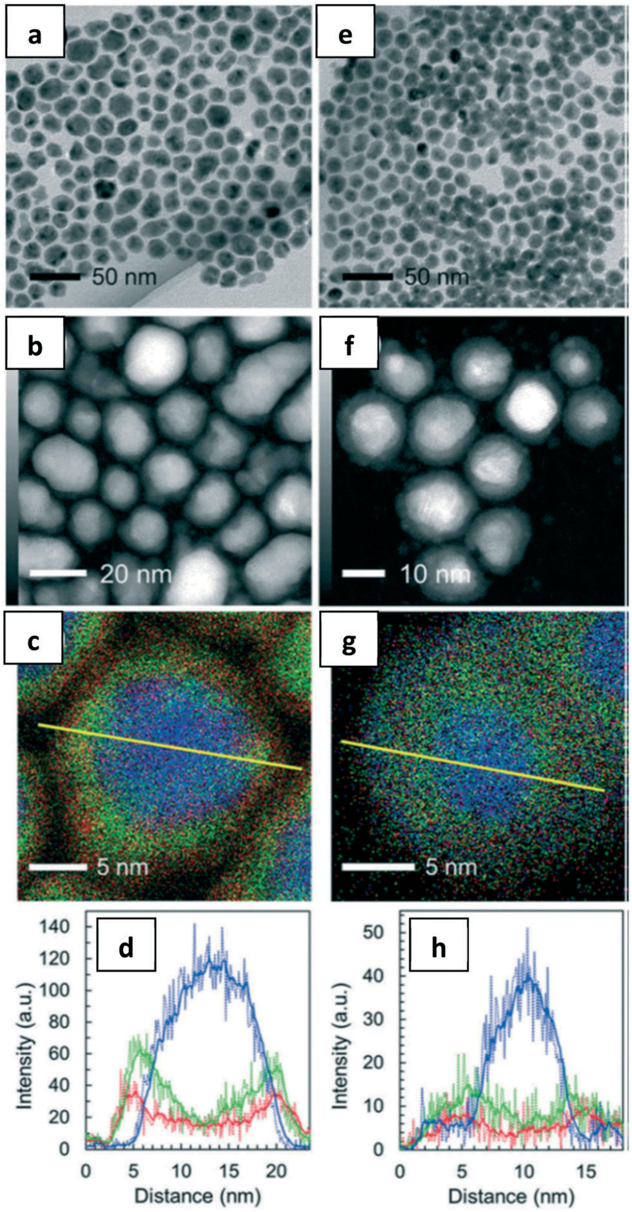

Fig. 5 Electron microscopic analysis of core–shell Ag@FeCo NPS (a–d) and core–shell–shell Ag@FeCo@Ag NPs (e–h). (a and e) TEM images, (b and f) STEM-HAADF images, (c and g) high-magnification EDS elemental mapping images of individual NPs and (d, h) line profiles of the yellow lines indicated in (c and g). Blue, red and green lines correspond to Ag L edge, Fe K edge and Co K edge, respectively. Reproduced with slight adaptation from ref. 39 with permission from the Royal Society of Chemistry.

Since core–shell structures are not limited to spherical shapes, other morphologies like cubic or rod-shaped core–shell systems are subject to extensive research.[40,41] Alternatively, core–shell structures may feature a non-uniform shell, which can be porous or nanostructured. In such cases, the core is still accessible, which often is beneficial for catalysis or electrochemical applications. As one example, Liu *et al.* presented the formation of featherlike structures which were composed of ZnO nanorods covered with a "shell" of Ni–Co layered double hydroxide (LDH) nanosheets.[42] This arrangement was realized *via* a two-step hydrothermal growth process, where first the ZnO nanorods were grown on a carbon cloth substrate and afterwards the Ni–Co LDH structures formed as nanosheets growing from the ZnO surface. The combination of both materials in a hierarchical structure led to

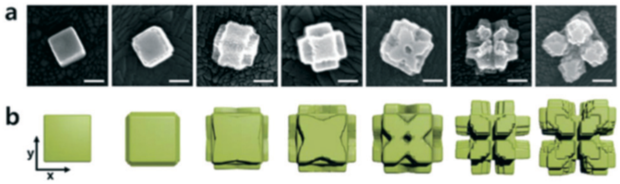

Fig. 6 (a) SEM images of Cu on Ag cubes at a cysteine concentration off 0 to 2 μM. The scale bars represent 100 nm. (b) Two-dimensional projections of the structural models. Reproduced from ref. 43 with permission from the Royal Society of Chemistry.

superior electrochemical performance when using the obtained product as electrode material in supercapacitors.[42]

Depending on the synthesis conditions, the deposition of a second phase however does not always preserve the morphology, but can even be utilized to create more complex structures. For example, Oh *et al.* used an electrodeposition technique to deposit copper on silver nanocubes.[43] As shape-directing agent they used cysteine which blocked the Cu {110} sites exclusively, and by varying the cysteine coverage on the Ag nanocubes, they formed a variety of structures including windmill, four-leaf clover and octapod-like structures (Fig. 6). The higher the cysteine coverage became, the more complex got the resulting structure.

On the other hand, already complex nanocrystals can be utilized as substrate for the growth of a second phase, creating even more complex structures. As an illustrative example reported by Lee *et al.*, concave PtZn cubes were synthesized in a hot mixture of stearic acid and octadecylamine in the presence of CO, and then a Au precursor was added (Fig. 7).[44] Whilst metallic Au is deposited in the center of the facets, filling the cavities, under inert atmosphere, the deposition preferably occurs at the corners of the PtZn cubes in CO atmosphere, resulting in multipods. Additionally, the morphology of the gold structure could be tuned by varying the reaction temperature and amount of gold precursor, which led to high control over the optical characteristics of the prepared materials, and in particular, their performance as substrates for surface-enhanced Raman spectroscopy (SERS).

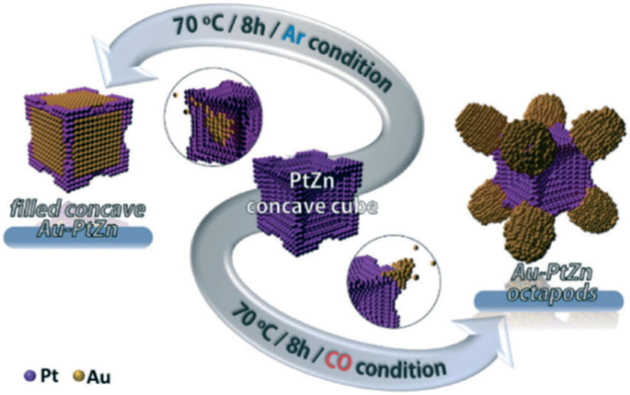

Fig. 7 Schematic diagram of the deposition of Au on PtZn concave nanocubes under different atmospheric conditions, resulting in Au–PtZn surface mosaic nanocubes (left) or Au–PtZn octapods (right). Reproduced from ref. 44 with permission from the Royal Society of Chemistry.

3. Nanocrystal formation

True nanocrystal engineering necessitates a comprehensive understanding of the underlying mechanisms of their formation. Hence, substantial research efforts are devoted to this topic, often involving specialized analytical methods. One aspect in this respect is the investigation and identification of intermediates in the formation process of nanocrystals. As a fascinating example, Mi *et al.* utilized total X-ray scattering to determine atomic distances in amorphous intermediates in the hydrothermal synthesis of TiO_2 nanoparticles.[45] Such hydrothermal or aqueous sol–gel approaches for the synthesis of metal oxides are still poorly understood. The scattering curves were transformed into pair distribution functions (PDFs) that served to reveal local ordering before and after crystallization (Fig. 8). Whilst the precursor was shown to be transformed *via* a solid-state-like reaction, the process was still strongly influenced by the solvent and the synthesis conditions, with initial nanocrystals possessing a high number of OH defects that decreased upon further growth. Whilst synchrotron-based total X-ray scattering thus showed to be a highly potent method to shed light on the formation process also before crystallization, a plethora of further methods can be utilized, including

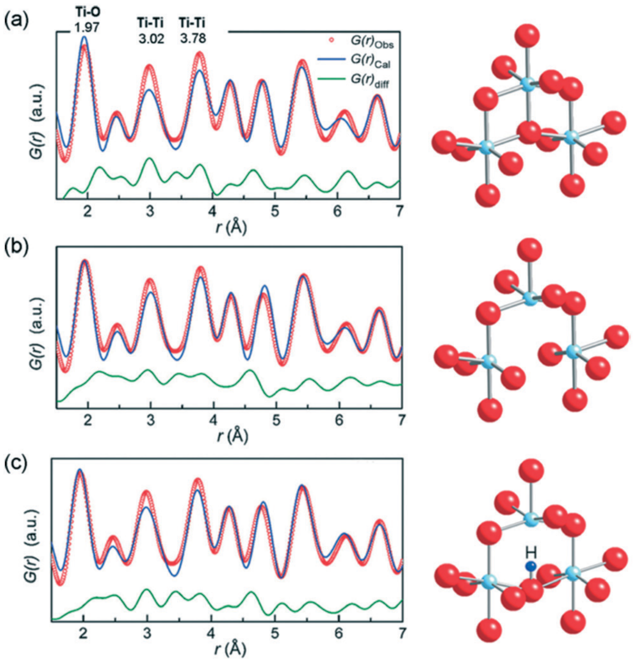

Fig. 8 Total X-ray scattering-based experimental, calculated and difference PDFs of TiO_2 nanocrystals, corresponding to an (a) anatase ordered structure; (b) anatase structure with oxygen vacancy; (c) anatase structure with OH defects; each with the corresponding structure model. Reproduced from ref. 45 with permission from the Royal Society of Chemistry.

chemical methods such as 2D-NMR spectroscopy, to identify novel intermediate states.[46]

Thorough investigations of particle formation processes increasingly involve studies on the kinetics of the overall process or the individual mechanistic steps, and alternatively on the influence of experimentally set dynamics on the product properties. Thereby, kinetics can be strongly different, and whilst for some nonaqueous synthesis processes of metal oxides, particle formation requires many hours or even a few days – although this can involve very fast steps after long reaction times due to self-catalyzed reactions[47] – in other cases changes in the range of seconds already lead to strong differences in the properties of the obtained nanocrystals.

Typically, reduction synthesis involves relatively fast kinetics, and even though such methods are relatively straightforward and well-controlled, there are many topical studies presenting novel insights into the reaction dynamics. For example, Gestraud *et al.* recently proved that a narrow time window needs to be realized for injection of the reducing agent in the synthesis of silver nanodisks for obtaining a highly monodisperse product.[48] For a similar synthesis, diffusion *vs.* reaction kinetics were identified to exert high influence on the morphology of the resulting product, ranging from fractal to spherical Ag and Cu nanostructures.[49]

Many studies provide highly fascinating insights into the formation kinetics by (directly or indirectly) monitoring the nucleation and growth of nanocrystals. Whilst the *ex situ* evaluation of samples withdrawn after different reaction times is broadly employed to deduce formation mechanisms,[50] methods for the direct *in situ* analysis of crystal growth at nanometer precision are becoming increasingly employed, in particular direct liquid-phase TEM monitoring.[51,52] On the other hand, the spectrum of suitable methods is continuously extended, especially *via* indirect methods such as NMR spectroscopy,[53] or small-angle X-ray scattering with increasing precision.[54–56]

Nanoparticle formation often involves non-classical mechanisms, in particular the oriented attachment of individual nanocrystals to larger units. Whilst this has been reported for many different materials and syntheses, with the probability of these mechanisms in high-temperature methods in organic solvents appearing to be particularly high, their general occurrence is still unclear. In the case of iron oxide and ferrite nanocrystals, for example, such fusion processes have been studied in detail for alcohol/polyol-based syntheses,[57,58] whilst AbuTalib *et al.* showed broader investigations on the impact of experimental conditions on the probability and extent of attachment processes for a thermal decomposition route.[59] The applicability of such insights for other systems remains to be seen. Thus, it appears that research efforts in the elucidation of nanocrystal formation and growth mechanisms will need to be intensified in the future to keep up with the rapid development of syntheses for novel types of nanomaterials and ultimately achieve a comprehensive understanding and broadly applicable models.

4. Superstructures

A different notion of nanocrystal engineering is the formation of ordered superstructures from individual nanoparticles. Notably, these do not need to be crystalline themselves, but crystallinity arises from their regular arrangement with defined periodicity in one, two, or all three dimensions. Whilst individual building blocks with rather uniform size and defined morphology are necessary, the main focus of engineering is on the arrangement process, typically achieved *via* self-assembly, to achieve high crystalline order, which depends on the utilized building units as well as the process parameters. A crucial aspect is the colloidal stabilization of the building blocks against processes like agglomeration and aggregation, as these would lead to irregular structures. Moreover, analogously to simple nanocrystals, crystalline superstructures, which we can call supercrystals, are characterized by their size and morphology, although these properties are of lower importance than for primary nanocrystals. Thereby, their dimensionality is a fundamental property that also has strong implications on the formation process – for example, 2D superstructures often are formed at interfaces, which is not directly possible for 3D structures. Within one class of supercrystals, the focus of most works is to obtain structures with highest ordering and sizes as large as possible, at least substantially larger than the individual building units. However, it can be expected that precise control of the size and shape of supercrystals will become more relevant in the future. One example is the formation of supraparticles, which are particle-type (often spherical) supercrystals that typically can be formed from droplets of suspensions of the primary particles.

4.1 Extended 2D and 3D Supercrystals

Whilst the formation of superlattices has been shown for a broad variety of materials as well as a multitude of morphologies, many fundamental aspects still have not been fully resolved yet. One example is the requirement of monodispersity for achieving crystalline packing for various shapes. In this respect, Theiss *et al.* investigated the self-assembly of hexagonally-shaped ZnO nanocrystals to 2D supercrystals, interestingly observing neither glass-to-crystal transition nor a critical polydispersity value limiting the crystallization.[60] Lee *et al.* studied the effect of morphology deviation on the formation of supercrystals of Ag polyhedra.[61] For strong differences in morphology, segregation was observed during the self-assembly process, which resulted in dual-structure supercrystals featuring phase boundaries; in this case the particles were about the same size and just differed in their shape.

Many studies were performed to investigate the role of the process parameters such as evaporation rates, solvent interactions and the role of solvent/solvent or solvent/air interfaces to create highly ordered 2D and 3D superstructures.[62–64] A remarkable finding was made by Hudait *et al.*, who reported the formation of "connections" of specific crystal facets of self-assembled polyhedral perovskite

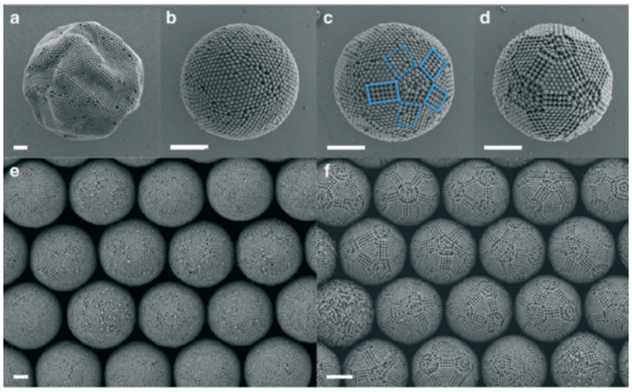

Fig. 9 Particle-type supercrystals from confined self-assembly of polystyrene beads in water-in-oil emulsion droplets. Four distinct cluster morphologies with increasing degree of ordering are observed: (a) buckled; (b) spherical clusters exhibiting only local order; (c) partial icosahedral clusters showing five-fold symmetry axes and incomplete faceting (dotted blue boxes); (d) icosahedral clusters with well-defined facets and complete icosahedral symmetry. (e and f) Low-magnification SEM images highlighting the uniformity in size and structure of the prepared clusters. Scale bars, 2 μm. Reproduced from ref. 66 under CC-BY 4.0 license, https://creativecommons.org/licenses/by/4.0/.

nanocrystals.[65] In this approach, during the drying process the perovskite crystals started to show oriented attachment and fusion of specific crystal faces, depending on their chemical composition. This process only took place on solid substrates but not in dispersion, and could be terminated by heating or ligand treatment.

4.2 Particle-type superstructures

The formation of particle-like supercrystals is typically achieved by spray-drying, or in microfluidic systems *via* the evaporation of droplets in an immiscible outer medium. *Via* the second strategy, highly defined crystals can be obtained, as *e.g.* presented by Wang *et al.*[66] In this study, monodisperse polystyrene beads were utilized to study so-called 'magic number clusters' that provide highly organized shells. Hence, not only the degree of ordering within the crystal, but also its ordering at the surface could be understood and modeled (Fig. 9).

The formation of such structures is highly dependent on the use of truly monodisperse building blocks. When primary particles of broader size distribution are used, not only the crystalline order deteriorates, but even a segregation effect of different particle sizes may occur.[67] Detailed insights on particle-type supercrystals are given in the review by Wintzheimer *et al.*[68]

4.3 Solution-based 3D supercrystals

Approaches leading to the formation of supercrystals in a liquid medium have been reported for many different materials and are highly attractive due to their good possibility of scale-up. Often, the self-assembly process is directly coupled to the synthesis in a one-pot approach, which offers high experimental simplicity,[69] but can also be achieved in a separate step.[70] Recently, fascinating works have presented possibilities of tuning the morphology of the resulting supercrystals simply *via* the chemical adjustment of the reaction conditions. Xu *et al.* presented an example on the controllability of the self-assembly of Pt-nanocrystals in a one-pot synthesis.[71] Thereby, a variety of superstructures with defined shapes were obtained when changing synthesis parameters like the used solvent, and adding surfactants and structure-directing agents (Fig. 10). Since the basic reaction procedure remained the same for all experiments, the

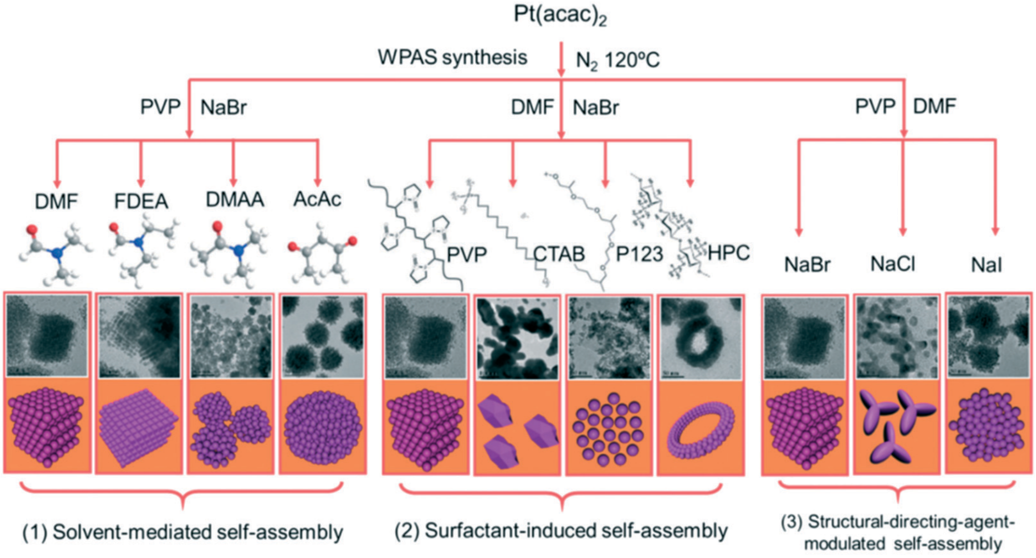

Fig. 10 Schematic illustration of the formation of 3D Pt nanocrystal superstructures obtained by solvent-mediated, surfactant-induced, and structure-directing-agent-modulated self-assembly processes using different solvents and surfactants as structure-directing agents. Reproduced from ref. 71 with permission from the Royal Society of Chemistry.

approach proved to give high flexibility, however not only the morphology of the supercrystals but also the properties of the formed primary nanocrystals changed for different experimental conditions.[71]

Analogously to the formation of primary particles the detailed investigation of formation mechanisms and kinetics of superstructures is of fundamental importance for their engineering and rational synthesis. In an attempt to monitor supercrystal formation in solution partially concurrent to the synthesis of $CsPbBr_3$ perovskite nanocrystals, Huang *et al.* realized an experimental setup to detect the change in photoluminescence, which was matched with results of SAXS.[72] After detailed analysis, nanocrystals of the same size were proposed to show high tendency to form assemblies, whilst nanocrystals larger or smaller than the majority of the product remained individual. According to the authors, the formation of such supercrystals is typical for perovskite syntheses, but due to the immediate redispersion in standard preparation processes the formed superstructures often are destroyed and even go unnoticed in many cases. This example shows that the understanding of supercrystal formation processes has substantially increased recently, and can be expected to facilitate and accelerate the advancement of synthetic approaches for supercrystals in the future.

Conclusion

Whilst nanocrystal engineering is less defined than the established field of crystal engineering applied on molecular solid state structures, this term has become increasingly used in the past two decades. CrystEngComm has published more than 2500 articles on nanomaterials since 2003, proving that scientists desire cross-disciplinary exchange of results on the design, formation, growth, and properties of nanocrystals in a designated forum of crystal engineering. In this Highlight article, we intended to provide an overview of the breadth of nanocrystal engineering with a focus on inorganic materials, by highlighting recent examples. We proposed nanocrystal engineering to involve both nanocrystals composed of atomic or molecular species and the assembly of supercrystals composed of nanoscale building blocks. Thereby, the different aspects cover a wide range of research topics. We showed that inorganic nanocrystals with increasing complexity have been synthesized, for example involving the combination of different materials to core–shell or core–multishell crystals as well as non-classical crystal morphologies. Also examples of hollow and concave nanocrystals that are highly relevant for applications *e.g.* in catalysis were presented, as their synthesis has received more and more attention in the last years.

Whilst research on nanocrystals is still largely empirical, a mechanistic understanding of crystal formation and growth processes is a key requirement for the future goal of true nanocrystal design for a specific application and the rational synthesis of pre-defined structures and morphologies. Significant advances in this direction have been made, ranging from the tailoring of morphologies for particular systems and the adaptation of phase composition to the investigation of the nanocrystal formation process itself. With respect to the latter, modern analytical tools have created tremendous possibilities in the last years, from the direct monitoring of crystal growth *via* liquid-cell TEM investigations to advanced spectroscopic and X-ray tools for *in situ* characterization of intermediate structures and their dynamics. Whilst great progress can be expected in the understanding and modeling of particle formation and growth processes in the near future, the development of unifying concepts and more broadly applicable models is a major task necessitating strong exchange between scientists from different fields in the framework of nanocrystal engineering.

Finally, high analogy between "traditional" crystal engineering of molecular solid state structures and the world of nanomaterials can be found in the ordered assembly of defined single nanocrystals to larger supercrystals. In both cases, the choice of the individual building blocks enables a design of crystals with desired properties. The field of molecular crystals also indicates what might lie ahead in the field of mesoscale supercrystals, in particular the tuning of morphology *via* certain building blocks – *e.g. via* the use of primary nanocrystals with specific morphologies – or the adjustment of mechanical properties by varying the interaction and spacing between the primary units. Fascinating possibilities could arise from the controlled assembly of complex primary nanocrystals, demonstrating the bright future of nanocrystal engineering. This work is intended to spark further discussion on the identity and scope of nanocrystal engineering. We hope that it will lead to enhanced prominence of this term, raising the awareness of the benefits and necessities of inter-system and cross-disciplinary exchange to advance this highly fascinating and fundamental research field.

Abbreviations

EDS/EDX	Energy dispersive X-ray spectroscopy
HAADF	High-angle annular dark-field imaging
NMR	Nuclear magnetic resonance
NPs	Nanoparticles
SERS	Surface-enhanced Raman spectroscopy
STEM	Scanning transmission electron microscopy
SAXS	Small-angle X-ray scattering
SEM	Scanning electron microscopy
TEM	Transmission electron microscopy

Author contributions

M. Görke and G. Garnweitner both contributed to the manuscript as writers. G. Garnweitner also conceived the work and acted as supervisor.

Conflicts of interest

There are no conflicts to declare.

Acknowledgements

M. Görke acknowledges support from the Hannover School for Nanotechnology.

References

1 G. R. Desiraju, *Crystal Engineering. The Design of Organic Solids*, Elsevier, Amsterdam, 1989.

2 Richard Zsigmondy, *Justus Liebigs Ann. Chem.*, 1898, 29–54.

3 J. Turkevich, P. C. Stevenson and J. Hillier, *Discuss. Faraday Soc.*, 1951, **11**, 55.

4 Z. Li, T. Chen, J. Chen, D. Sun, L. Liu, M. Liu and Y. Lu, *CrystEngComm*, 2017, **19**, 7001–7008.

5 W. Qin and L. Zhu, *Sci. Rep.*, 2020, 13904.

6 Y. Qin, Y. Lu, D. Yu and J. Zhou, *CrystEngComm*, 2019, **21**, 5602–5609.

7 T.-H. Yang, S. Zhou, K. D. Gilroy, L. Figueroa-Cosme, Y.-H. Lee, J.-M. Wu and Y. Xia, *Proc. Natl. Acad. Sci. U. S. A.*, 2017, **114**, 13619–13624.

8 M. Zhang, J. Yu, J. Zhang, Q. Lan, J. Dai, Y. Huang, G. Li, Q. Fan, X. Fan and Z. Zhou, *Chem. Phys. Lett.*, 2017, **671**, 154–160.

9 M. Kang, H. Zhou, D. Wu and B. Lv, *CrystEngComm*, 2016, **18**, 9299–9306.

10 Y. Tian, X. Lian, Y. Wu, W. Guo and S. Wang, *CrystEngComm*, 2020, **22**, 5218–5225.

11 S. Zellmer, A. Kockmann, I. Dosch, B. Temel and G. Garnweitner, *CrystEngComm*, 2015, **17**, 6878–6883.

12 Q. Zhu, Z. Zhang, Y. Lv, X. Chen, Z. Wu, S. Wang and Y. Zou, *CrystEngComm*, 2019, **21**, 4568–4577.

13 F. Besenbacher, M. Brorson, B. S. Clausen, S. Helveg, B. Hinnemann, J. Kibsgaard, J. V. Lauritsen, P. G. Moses, J. K. Nørskov and H. Topsøe, *Catal. Today*, 2008, **130**, 86–96.

14 N. Kondekar, M. G. Boebinger, M. Tian, M. H. Kirmani and M. T. McDowell, *ACS Nano*, 2019, **13**, 7117–7126.

15 X. Chen, K. Zhang, Y. Yang, K. Yang, Q. Fan, C. Yu, W. Huang and W. Dai, *CrystEngComm*, 2020, **22**, 6699–6712.

16 T. Zhou, M. Hu, J. He, R. Xie, C. An, C. Li and J. Luo, *CrystEngComm*, 2019, **21**, 5526–5532.

17 D. Yu, T. Jiang, F. Wang, Z. Wang, Y. Wang, W. Shi and X. Sun, *CrystEngComm*, 2009, **11**, 1270–1274.

18 S. Thakur and S. K. Mandal, *Mater. Adv.*, 2021, **2**, 511–524.

19 R. E. Nikolaev, V. S. Sulyaeva, A. V. Alekseev, A. S. Sukhikh, E. V. Polyakova, T. A. Pomelova, T. Kuzuya, S. Hirai and B. T. Nhu, *CrystEngComm*, 2021, **23**, 2196–2201.

20 N. H. de Leeuw and J. A. L. Rabone, *CrystEngComm*, 2007, **9**, 1178–1186.

21 Y. Zhao, W. Wang, M. Chen, R. Wang and Z. Fang, *CrystEngComm*, 2018, **20**, 7266–7274.

22 R. Zhao, Z. Chen and S. Huang, *CrystEngComm*, 2020, **22**, 1586–1592.

23 T.-T. Lv, H.-X. Wang, X.-B. Ren, L.-C. Wang, R.-M. Ding, J.-P. Cao and B.-L. Lv, *CrystEngComm*, 2020, **22**, 8214–8220.

24 J. Yang, L. Wei, T. Zhao, T. Yang, J. Wang, W. Wu, X. Yang, Z. Li and M. Wu, *Electrochim. Acta*, 2019, **318**, 949–956.

25 Y. Zhang, R. Shi, J. Ren, Y. Dai, Y. Yuan and Z. Wang, *Langmuir*, 2019, **35**, 16752–16760.

26 P.-E. Rouet, C. Chomette, E. Duguet and S. Ravaine, *Angew. Chem., Int. Ed.*, 2018, **57**, 15754–15757.

27 Z. Li, X. Wang, Z. Zhang, J. Hu, Z. Liu, D. Sun and Y. Tang, *CrystEngComm*, 2020, **22**, 1541–1546.

28 W. Tong, B. Huang, P. Wang, L. Li, Q. Shao and X. Huang, *Angew. Chem., Int. Ed.*, 2020, **59**, 2649–2653.

29 T. Kollek and S. Polarz, *CrystEngComm*, 2017, **19**, 4615–4621.

30 F. Panciera, Z. Baraissov, G. Patriarche, V. G. Dubrovskii, F. Glas, L. Travers, U. Mirsaidov and J.-C. Harmand, *Nano Lett.*, 2020, **20**, 1669–1675.

31 B. A. Tappan, M. K. Horton and R. L. Brutchey, *Chem. Mater.*, 2020, **32**, 2935–2945.

32 W. He, J. Hu, C. Chen, Y. Chen, L. Zeng, X. Zhang, B. Cai, Y. Mai and F. Guo, *ACS Appl. Mater. Interfaces*, 2020, **12**, 55830–55837.

33 D. Baek, T. K. Lee, I. Jeon, S. H. Joo, S. Shin, J. Park, S. J. Kang, S. K. Kwak and J. Lee, *Adv. Sci.*, 2020, **7**, 2000104.

34 T. A. Cheema and G. Garnweitner, *CrystEngComm*, 2014, **16**, 3366–3375.

35 P. Stolzenburg and G. Garnweitner, *React. Chem. Eng.*, 2017, **2**, 337–348.

36 M. S. Santos, J. C. C. Freitas and C. J. Dalmaschio, *CrystEngComm*, 2020, **22**, 1802–1811.

37 Y. Yu, G.-H. Nam, Q. He, X.-J. Wu, K. Zhang, Z. Yang, J. Chen, Q. Ma, M. Zhao, Z. Liu, F.-R. Ran, X. Wang, H. Li, X. Huang, B. Li, Q. Xiong, Q. Zhang, Z. Liu, L. Gu, Y. Du, W. Huang and H. Zhang, *Nat. Chem.*, 2018, **10**, 638–643.

38 M. Sun, X. Fu, K. Chen and H. Wang, *ACS Appl. Mater. Interfaces*, 2020, **12**, 46146–46161.

39 M. Takahashi, K. Higashimine, P. Mohan, D. M. Mott and S. Maenosono, *CrystEngComm*, 2015, **17**, 6923–6929.

40 S. F. Tan, G. Bisht, U. Anand, M. Bosman, X. E. Yong and U. Mirsaidov, *J. Am. Chem. Soc.*, 2018, **140**, 11680–11685.

41 S. F. Tan, S. W. Chee, G. Lin, M. Bosman, M. Lin, U. Mirsaidov and C. A. Nijhuis, *J. Am. Chem. Soc.*, 2016, **138**, 5190–5193.

42 X. Liu, H. Liu and X. Sun, *CrystEngComm*, 2020, **22**, 1593–1601.

43 H. Oh, H. Hwang and H. Song, *Nanoscale*, 2021, **13**, 1777–1783.

44 K. W. Lee, H. An, S. Haam, H. Baik and K. Lee, *CrystEngComm*, 2015, **17**, 6838–6842.

45 J.-L. Mi, K. M. Ø. Jensen, C. Tyrsted, M. Bremholm and B. B. Iversen, *CrystEngComm*, 2015, **17**, 6868–6877.

46 M. Zimmermann, K. Ibrom, P. G. Jones and G. Garnweitner, *ChemNanoMat*, 2016, **2**, 1073–1076.

47 M. Zimmermann and G. Garnweitner, *CrystEngComm*, 2012, **14**, 8562–8568.

48 C. Gestraud, P. Roblin, J. F. Morris, M. Meireles and Y. Hallez, *CrystEngComm*, 2020, **22**, 1769–1778.

49 T. Yang, J. Liu, J. Dai and Y. Han, *CrystEngComm*, 2017, **19**, 72–79.

50 Q. Sun, Y. Zeng and D. Jiang, *CrystEngComm*, 2012, **14**, 1595–1601.

51 W. Wei, T. Bai, R. Fu, L. Sun, W. Wang, M. Dong, L. Chen, Z. Guo and F. Xu, *Nanoscale*, 2021, **13**, 3136–3143.

52 M. Dong, R. Fu, H. Min, Q. Zhang, H. Dong, Y. Pan, L. Sun, W. Wei, M. Qin, Z. Zhu and F. Xu, *Cryst. Growth Des.*, 2021, **21**, 1314–1322.

53 R. Mashiach, H. Weissman, L. Avram, L. Houben, O. Brontvein, A. Lavie, V. Arunachalam, M. Leskes, B. Rybtchinski and A. Bar-Shir, *Nat. Commun.*, 2021, **12**, 229.

54 J. Polte, R. Erler, A. F. Thünemann, S. Sokolov, T. T. Ahner, K. Rademann, F. Emmerling and R. Kraehnert, *ACS Nano*, 2010, **4**, 1076–1082.

55 X. Chen, J. Wang, R. Pan, S. Roth and S. Förster, *J. Phys. Chem. C*, 2021, **125**, 1087–1095.

56 J. C. Porsiel, B. Temel, A. Schirmacher, E. Buhr and G. Garnweitner, *Nano Res.*, 2019, **12**, 2849–2857.

57 I.-C. Masthoff, A. Gutsche, H. Nirschl and G. Garnweitner, *CrystEngComm*, 2015, **17**, 2464–2470.

58 T. Gaudisson, S. K. Sharma, R. Mohamed, B. Sitamtze Youmbi, N. Menguy, F. Calvayrac, M. Seydou and S. Ammar-Merah, *CrystEngComm*, 2021, **23**, 1756–1764.

59 N. H. AbuTalib, A. P. LaGrow, M. O. Besenhard, O. Bondarchuk, A. Sergides, S. Famiani, L. P. Ferreira, M. M. Cruz, A. Gavriilidis and N. T. K. Thanh, *CrystEngComm*, 2021, **23**, 550–561.

60 S. Theiss, M. Voggel, M. Schlötter, S. Sutter, M. T. Stöckl and S. Polarz, *CrystEngComm*, 2019, **21**, 5137–5144.

61 Y. H. Lee, C. L. Lay, W. Shi, H. K. Lee, Y. Yang, S. Li and X. Y. Ling, *Nat. Commun.*, 2018, **9**, 2769.

62 X. Huang, J. Zhu, B. Ge, K. Deng, X. Wu, T. Xiao, T. Jiang, Z. Quan, Y. C. Cao and Z. Wang, *J. Am. Chem. Soc.*, 2019, **141**, 3198–3206.

63 E. Marino, A. W. Keller, D. An, S. van Dongen, T. E. Kodger, K. E. MacArthur, M. Heggen, C. R. Kagan, C. B. Murray and P. Schall, *J. Phys. Chem. C*, 2020, **124**, 11256–11264.

64 Y. Liu, K. Deng, J. Yang, X. Wu, X. Fan, M. Tang and Z. Quan, *Chem. Sci.*, 2020, **11**, 4065–4073.

65 B. Hudait, S. K. Dutta, A. Patra, D. Nasipuri and N. Pradhan, *J. Am. Chem. Soc.*, 2020, 7207–7217.

66 J. Wang, C. F. Mbah, T. Przybilla, B. Apeleo Zubiri, E. Spiecker, M. Engel and N. Vogel, *Nat. Commun.*, 2018, **9**, 5259.

67 S. Zellmer, G. Garnweitner, T. Breinlinger, T. Kraft and C. Schilde, *ACS Nano*, 2015, **9**, 10749–10757.

68 S. Wintzheimer, T. Granath, M. Oppmann, T. Kister, T. Thai, T. Kraus, N. Vogel and K. Mandel, *ACS Nano*, 2018, **12**, 5093–5120.

69 A. Pucci, M.-G. Willinger, F. Liu, X. Zeng, V. Rebuttini, G. Clavel, X. Bai, G. Ungar and N. Pinna, *ACS Nano*, 2012, **6**, 4382–4391.

70 A. Tanaka, H. Kamikubo, M. Kataoka, Y. Hasegawa and T. Kawai, *Langmuir*, 2011, **27**, 104–108.

71 G. Xu, J. Liu, B. Liu and J. Zhang, *CrystEngComm*, 2019, **21**, 411–419.

72 H. Huang, M. W. Feil, S. Fuchs, T. Debnath, A. F. Richter, Y. Tong, L. Wu, Y. Wang, M. Döblinger and B. Nickel, *Chem. Mater.*, 2020, **32**, 8877–8884.